

# Lasers Technology



Lasers Development	12
Lasers Applications	15
High Intensity Lasers	19

# introduction

The **Laser Technology Program** of IPEN is developed by the Center for Lasers and Applications (CLA) and is committed to the development of new lasers based on the research of new optical materials and new resonator technologies. Laser applications and research occur within several areas such as Nuclear, Medicine, Dentistry, Industry, Environment and Advanced Research. Additional goals of the Program are human resource development and innovation, in association with Brazilian Universities and commercial partners.

The Program is divided into two main areas: “Material and Laser Development” that includes crystal growth of optical materials, characterization, modeling and optical spectroscopy of solids, plasmas and biological materials and the development of compact, highly efficient, diode pumped-solid state lasers.

The other main area, “Laser Applications”, is related to technological applications such as laser processing, laser remote sensing, development of new diagnostic and therapeutic methods like optical coherence tomography (OCT), laser Doppler flowmetry, photosensitization, prevention of dental caries and other advanced applications of high intensity lasers.

One of the biggest labs of the Center for Lasers and Applications uses a terawatt-laser for many of the above applications and also for basic research. Recent activities are highlighted below:

- Development of single crystal fibers for compact laser systems;
- Growth of a solid solution  $\text{LiGd}_{0.232}\text{Lu}_{0.75}\text{Nd}_{0.018}\text{F}_4:\text{Nd}$  crystal suitable to obtain a laser medium for mode-locking purposes;
- Characterization, modeling and optical spectroscopy of rare-earth doped crystals and glasses for the development of solid laser medium;
- First single crystal Nd:YLF fiber laser;
- Evaluation of the performance of laser-induced Breakdown Spectroscopy (LIBS) for the characterization of nuclear/radioactive materials;
- New method for the evaluation of microvascular functionality using low - frequency fluctuations in the laser Doppler flow signal;
- Construction of an automatized workstation with ultra short laser pulses (femtoseconds) for the study of thermal and non-thermal processes in dielectrics, semiconductors and metals;
- Study of a therapeutic method combining Nd:YAG laser and topical fluoride treatment for effective reduction of caries incidence in patient;
- Development of studies showing that photodynamic antimicrobial therapy is able to reduce 99% of multi-resistant bacteria in burn wounds;
- Analysis of Optical Coherent Tomography applied to dermatology (research work winner of the Natura Campus 2010 Premium for Technological Innovation);
- New LIDAR system for Industrial Emission and Detection installed in Cubatão/SP (collaboration in The National Institutes of Science and Technology Program /INCT);
- Studies for isotope enrichment by ultra short laser pulses.

### Crystal growth activities

The Crystal Growth Laboratory works on bulk, micro and nanocrystals research for materials properties studies and development of new lasers systems. The research for the development of laser crystals growth, with the desired properties includes: development of synthesis process, thermodynamic modeling of phase diagrams, instrumentation improvement, as well the study of the growth process itself. The research performed in this period was supported by CNPq, Fapesp and CAPES, including students fellowships and granted projects, in collaboration with Federal University of Sergipe and Federal University of Pernambuco (CNPq-INCT program in National Institute for Science and Technology in Photonics) in Brazil, the Leibniz Institute for Crystal Growth (Germany) and University of Lorraine (France).

### Phase diagrams

It is well known that phase diagrams data are essential for crystal growth process. Although the experimental phase diagram of some fluoride systems are already published there are scarce data concerning thermodynamic properties of such materials and frequently misunderstanding of results as a result of the easy contamination of fluorides by oxygen and moisture during experimental measurements.

In view of the interest in technological applications of some fluorides as active laser media, phase diagram of the systems LiF-YF<sub>3</sub>, GdF<sub>3</sub>-YF<sub>3</sub> and the ternary system LiF-GdF<sub>3</sub>-LuF<sub>3</sub> (interesting for LiReF<sub>4</sub> crystals growth, Re = Gd and/or Y, Lu) were studied by experimental and computational methods, using mainly differential scanning calorimetry (DSC) and the commercial simulation program FactSage, respectively. In both cases the resulting theoretical phase diagrams showed satisfactory agreement compared to the experimental ones. Specific heat capacity and enthalpy of phase transitions and fusion were measured and compared to published data.

Differential thermal analysis (DTA) of the LiF-BiF<sub>3</sub> system was also performed as a preliminary step for future studies on BiLiF<sub>4</sub> crystal growth. This matrix could be potentially interesting for opto-electronic applications, such as laser devices or scintillation detectors for photons. However, significant difficulties are reported in the literature to the growth of BiLiF<sub>4</sub>. Differential thermal analysis and x-ray diffraction analysis showed that melts with high bismuth fluoride concentration suffered from high evaporation; nevertheless even pure BiF<sub>3</sub> could be molten at 655°C. The system contains one intermediate compound BiLiF<sub>4</sub> which melts by peritectic decomposition with the formation of LiF at 450°C (Figure 1). The eutectic between BiLiF<sub>4</sub> and BiF<sub>3</sub> melts at 415°C. Thermodynamic assessment yielded  $c_p = 166.173 - 0.01072 T$  (in J mol<sup>-1</sup> K<sup>-1</sup>) for BiLiF<sub>4</sub>.

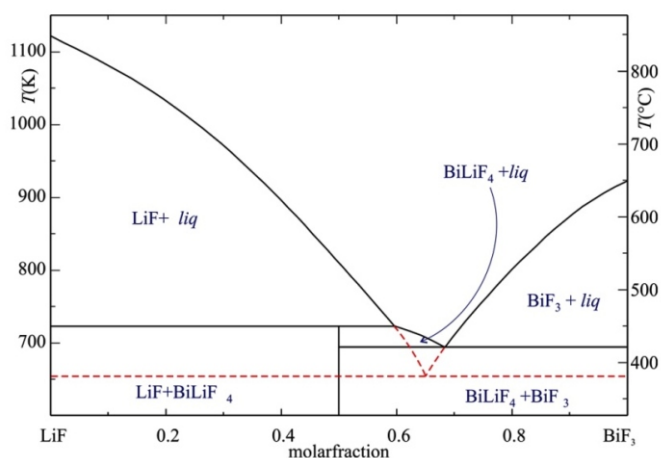


Figure 1. Theoretical phase diagram of LiF-BiF<sub>3</sub> system obtained with Factsage software\*.

### Bulk crystals

The year of 2013 was dedicated to Prof. Jan Czochralski, the scientist who developed one of the most important crystal growth methods which received his name. The Czochralski (CZ) method fitted very well in the past 50 years to the development of bulk laser crystals once it allows the grown of large oriented boules, with the high optical perfection required for the solid state lasers and other optical applications, being until nowadays the most commonly used process for crystal growth. The Crystal Growth Laboratory at CLA has a large experience with CZ fluoride bulk laser crystals grown for optical applications. A short review of our activities in the last 25 years was published in the Special Anniversary Issue dedicated to Professor Jan Czochralski Year, 2013, at the scientific journal *Acta Physica Polonica*.

Nd:YLiF<sub>4</sub> (Nd:YLF) crystals grown by the CZ method in our laboratories were also employed to obtain lasers with new features. A diode-side-pumped and passively Q-switched Nd:YLF laser operating at 1053 nm using a new laser resonator concept was reported on January 2012.

Another study with macro single crystals was developed in collaboration with the Federal University of Sergipe. Single crystals of BaY<sub>2</sub>F<sub>8</sub> (BYF) doped with different concentrations of Er<sup>3+</sup> and Tm<sup>3+</sup> were prepared by the Zone melting method under HF atmosphere. Optical characterization was performed with powder samples prepared by grinding the obtained ultra-pure crystals (only the grains from 38 μm to 63 μm diameters were used). The study concluded that this matrix doped with Er<sup>3+</sup> and Tm<sup>3+</sup> is an interesting material for radiation detection.

### Micro and nano crystals

In 2004 we started a program on single fiber growth by the micro-pulling down (μ-PD) method aiming the development of laser materials. Several fluoride materials has been studied (Nd and Er:YLF, Nd:BYF and BaLiF<sub>3</sub>). From 2009, we started investigations of tungstate laser crystals as single crystal fibers including the growth and characterization of Nd:NaLa(WO<sub>4</sub>)<sub>2</sub> (Nd:NLW), Nd:NaGd(WO<sub>4</sub>)<sub>2</sub> (Nd:NGW) and Nd doped LiLa(WO<sub>4</sub>)<sub>2</sub> (Nd:LLW). In the period the growth, structural and optical characterization of Eu:LiLa(WO<sub>4</sub>)<sub>2</sub> (Eu:LLW) and Nd:LiLa(MoO<sub>4</sub>)<sub>2</sub> (Nd:LLM) single crystal fibers were performed. For the first time, transparent and uniform in diameter, single crystal fibers of Eu:LLW and LiEu(WO<sub>4</sub>)<sub>2</sub> (LEW) were grown by the μ-PD method. Eu:LLW single crystal fibers present strong red emission under 395 nm excitation with an observed concentration quenching of around 20 mol% of doping. Excitation spectroscopy experiments showed that the symmetry S<sub>4</sub> of the point site is occupied by Eu<sup>3+</sup> when it partially or totally (LEW case) replaces La<sup>3+</sup> in the LLW fiber crystals. Eu:LLW crystal fibers reveals itself as a promising matrix for developing near-UV convertible luminescent devices in the red range.

In cooperation with Federal University of Sergipe computer modelling of the undoped and Eu<sup>3+</sup>-doped LLW structure was successfully achieved by energy minimization and mean field theory. The results were compared with experimental data previously published and are in good agreement with them. A linear regression of the lattice parameters was also proposed as a function of the dopant concentration. Regarding the optical luminescence, the concentration limit of Eu doping was also determined.

Undoped and Nd -doped LLM single crystal fibers were characterized concerning their structural and spectroscopic properties. First the optimization of the growth conditions was studied in order to avoid facet formation. The grown fibers are free of scattering centers and the real dopant concentration was confirmed to be very close to the nominal ones by micro X-ray fluorescence with Synchrotron radiation, in experiments performed at LNLS - Campinas, Brazil. Quite uniform distributions along the fibers length were observed. The crystallographic structure concerning the scheelite tetragonal symmetries was re-evaluated. Selective laser excitation of the <sup>4</sup>F<sub>3/2</sub> at 875 nm and <sup>4</sup>F<sub>5/2</sub> at 805 nm has established that the energy levels above

the  ${}^4F_{3/2}$  level are entirely quenched by multiphonon emission in Nd:LLM crystal fiber. The potential laser gain of the system was determined using a numerical solution of the rate equations system for the 805 nm continuous pumping regime, which shows the maximum gain of the laser emission at 1.064 microns for using a  $\text{Nd}^{3+}$ -doping of 5 mol%.

The preparation Nd, Yb -doped LLM as single powder by polymerized complex method was also experienced for future random laser studies. The pH control effect on the preparation of Nd:LLW 1.0 mol% microcrystals in the powder shape was evaluated. The samples contained mostly the LLW phase showing irregular morphology and agglomerates with average sizes of 22-48  $\mu\text{m}$ . The effect (in the increase of the agglomerates size) of the calcination temperature is higher than of the calcination time.

### Development of compact diode-pumped solid-state laser sources

This activity comprises the development of new laser sources based on diode pumped solid state lasers (DPSSL) for applications in research, industry, medical and pollution control. Our investigations are focused mainly on controlling the temporal, spectral and spatial features of the laser beam. In some cases it also includes the production design of such systems including the reliability tests and application experiments. We have built several DPSSL systems emitting from the blue up to the far infrared.

We have developed several proprietary designs, the most important being called DBMC (double-beam mode controlling), that have resulted in extremely efficient and compact diode-laser with up to several tens of watts of output power in continuous (cw) operation. Some highlights of the last period are shown below:

- The highest efficiencies for diode pumped Nd:YLF lasers reported so far was achieved: 53.6% at 1053 nm in a side pumped configuration in cw operation, but also at 1313 nm and in Q-switched operation.

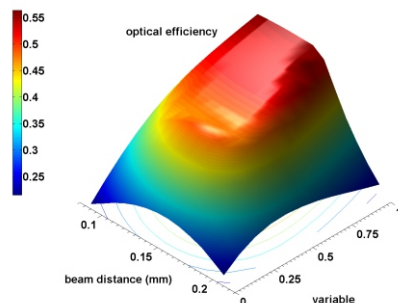


Figure 2. Simulation of the efficiency in a diode side-pumped laser using DBMC technology as a function of alignment and spectroscopic parameters.

- For the first time, a compact, diode-pumped  $\text{Nd}^{3+}$ :YLF Raman lasers operating at the first Stokes of 1163 nm with frequency doubling into the lime-yellow and orange frequency range and of watt-level continuous output was built. The achieved wavelengths are 549 nm (0.65 W), 552 nm (1.9 W), 573 nm (0.6 W) and 581 nm (1.1 W).

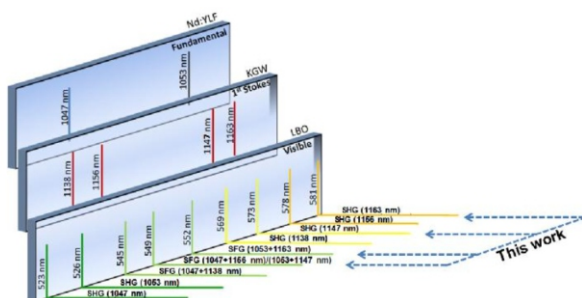


Figure 3. Wavelength that can be generated using the combination of Nd:YLF/KGW/LBO.

- Random lasing in nanocrystalline Nd:YVO powder was demonstrated for the first time and a method that analyzes the decay kinetics after long-pulse excitation was used to determine the laser characteristics. This method permits to measure the fractional contribution of spontaneous and stimulated emission as well as upconversion as a function of the pump intensity. We observed that maximum linewidth narrowing is achieved when the stimulated emission reaches 50% of fractional contribution in the backscattering cone.

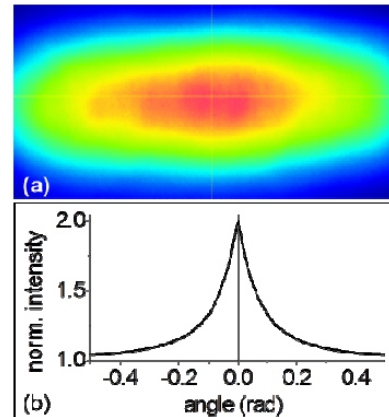


Figure 4. Backscattered cone of 1064 nm emission (a), obtained using a CCD digital camera. (b) Simulation of the coherent backscattered emission from this sample.

### Characterization, modeling and optical spectroscopy of rare-earth doped solid laser media

A luminescence spectroscopic system with spectral and temporal discrimination that uses a Box-car technique and tuneable laser excitations of 4 ns (10 Hz) in the range of 420 to 2000 nm (10mJ) was used for lifetime measurements of rare earth ions in glasses and fluorides crystals. These measurements allowed determining the rate constant of the non-radiative energy transfer that happens due to multipolar interactions between donor and acceptor ions in solids. Energy transfer mechanism involving two interacting erbium (and holmium) ions in the first (and second) excited state, energy-transfer up-conversion have been observed and the rate constant determined. The aim of this study is the development of solid laser medium emitting in the near to mid-infrared (1400 - 3600 nm) and to improve light signal amplifiers based on thulium-doped materials that operate in S-band of telecommunication (1470 - 1500 nm). A detailed investigation of the energy transfer process from the first excited state of holmium caused by  $\text{Pr}^{3+}$  ions in fluorozirconate (ZBLAN) glass was carried out, resulting in the development of a 1W diode-pumped tuneable  $\text{Ho}^{3+}$ ,  $\text{Pr}^{3+}$ -doped fluoride glass fibre laser emitting 2830 – 2950 nm.

Solving the rate equations describing the mechanisms involved in the optical cycle of a laser transition one can verify the potential gain of the laser emission and know how it can be affected by dopant concentration (activator and sensitizer ions) and pumping intensity.

Tellurite glasses doped with 0.5, 1, 2, 3 mol% of  $\text{Dy}^{3+}$  were investigated using the time-resolved luminescence spectroscopy. Selective laser excitation at 805 and 1300 nm established that the energy levels above the second excited state of  $\text{Dy}^{3+}$  are entirely quenched by non-radiative multiphonon emission in tellurite glass. Only two emissions are present with peaks at 1700 nm and 2890 nm with low quantum efficiencies. The luminescence decay of the  ${}^6\text{H}_{13/2}$  level exhibits two distinct components (with decay time values of 20  $\mu\text{s}$  and 112  $\mu\text{s}$ ) in  $\text{Dy}^{3+}$  (1 mol%)-doped TZNF in contrast with the single exponential decay (with a decay time of 9.7  $\mu\text{s}$ ) measured for  $\text{Dy}^{3+}$  (3 mol%)-doped TZNF. Increasing the  $\text{ZnF}_2$  component to 20 mol% in the TZNF glass host may lead to a larger contribution by the longer time component to the overall decay of laser level emitter ( ${}^6\text{H}_{13/2}$ ). Our numerical simulation suggested that  $\text{Dy}^{3+}$  (1 mol%)-doped TZNF may exhibit a population inversion for laser emission at 3042 nm

when the pump threshold, for 1300 nm light, of  $15 \text{ kW cm}^{-2}$  is exceeded.

ZBLAN glasses doped with 1 mol% of  $\text{Pr}^{3+}$  and co-doped with 1, 2, 3, 4 and 5 mol% of  $\text{Yb}^{3+}$  were investigated using the time-resolved luminescence spectroscopy. Selective laser excitation at 970 nm established that forward  $\text{Yb}^{3+} \rightarrow \text{Pr}^{3+}$  ET has two components: a fast component that accounts for 45% of the total transfer and a slow component that accounts for 55%. Forward ET should be assisted by hopping migration. We observed upconversion processes between  $\text{Yb}^{3+}$  and  $\text{Pr}^{3+}$  ions whose rate  $W_{\text{up}}$  (in  $\text{s}^{-1}$ ) is dependent on  $[\text{Yb}^{3+}]$ . It was established that upconversion to the  $^3\text{P}_0$  excited state of  $\text{Pr}^{3+}$  may have a small detrimental impact on the performance of a  $\text{Yb}^{3+}$ ,  $\text{Pr}^{3+}$ -doped ZBLAN fiber laser when CW pumped at 975 nm. We have found that the  $\text{Yb}^{3+}$  (1 mol%),  $\text{Pr}^{3+}$  (1 mol%) is the most efficient sample for laser emission at 3650 nm within the  $\text{Yb}^{3+}$  concentration range 1 to 5 mol%. This dopant combination can be applied to the three main emissions that start from the  $^1\text{G}_4$  level ( $\text{Pr}^{3+}$ ) and that terminate on the  $^3\text{H}_5$ ,  $^3\text{H}_6$ , and  $^3\text{F}_4$  energy levels and emit at 1350, 1985, and 3680 nm, respectively. All these emissions have laser potential with a positive small signal gain with a negligible threshold pumping intensity, which indicates that  $\text{Pr}^{3+}$ ,  $\text{Yb}^{3+}$ -codoped ZBLAN glass is a promising candidate for high power laser operation at 3650 nm using diode laser pumping at 975 nm.

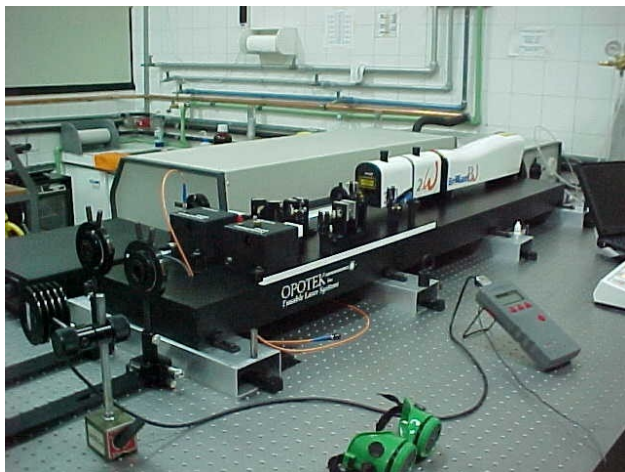


Figure 5. The decay characteristics of the excited states of rare earth ions were measured using a pulsed (4 ns) laser excitation from a tunable double optical parametric oscillator (OPO) pumped by the third (or second) harmonic of a Q-switched Nd:YAG laser working in the visible (420 to 685 nm) and in the infrared in two spectral ranges: (1) 670 to 990 nm and (2) 1150 to 2050 nm.

### Time of correlation of low-frequency fluctuations in the regional laser Doppler flow signal from human skin

The laser Doppler flowmetry allows the non-invasive assessment of the skin perfusion in real-time, being an attractive technique to study the human microcirculation in clinical settings. Low-frequency oscillations in the laser Doppler blood flow signal from the skin have been related to the endothelial, neurogenic and myogenic mechanisms of microvascular flow control, in the range 0.0095-0.02 Hz, 0.02-0.06 Hz and 0.06-0.16 Hz respectively. The mean Amplitude of the periodic fluctuations in the laser Doppler blood flow signal, in each frequency range, derived from the respective wavelet-transformed coefficients, has been used to assess the function and dysfunctions of each mechanism of flow control. Known sources of flow signal variances include spatial, temporal and inter-individual variability, diminishing the discriminatory capability of the technique. A new time domain method of analysis was developed, based on the Time of Correlation (TC) of flow fluctuations between two adjacent sites. Registers of blood flow from two adjacent regions, for local temperature of 32 degrees Celsius (baseline) and thermally stimulated (42 degrees Celsius) of volar forearms from 20 healthy volunteers were collected and analyzed. The results obtained revealed high time of correlation between two adjacent regions when thermally stimulated, for signals in the endothelial, neurogenic and myogenic frequency ranges. Experimental data also indicate lower variability for TC when compared to the mean amplitude of the Doppler signal, suggesting a new promising parameter for assessment of the microvascular flow control.

### Laser processing technics: thermal and non-thermal process

Modern technological advances have demanded the development of new materials like high mechanical strength steels, superalloys, ceramics and composites, besides very small pieces with complex geometrical forms. Consequently, traditional milling and welding processes can no longer fulfill the requirements demanded by modern applications. Hence, laser processing comes as very useful and versatile alternative method, and has been used here for cutting welding, heat treating and ablating of many materials for important technological applications.

In welding, a pulsed Nd:YAG laser has been used to produce an effective protection of the control element against contact with water inside the pool of the IPEN's nuclear reactor IEA-R1. This has been done by means of a protective envelope of stainless steel precisely welded around the element slab. This technique has been also used to join very thin foils of alloys that are highly resistant to corrosion with the purpose of using them as protective shields for sensors against harsh media. Pressure, flow and temperature sensors used in many industrial and nuclear plants must withstand extreme conditions of pressure, temperature and corrosive environments. This is done by covering these devices with foils of special alloys with 100  $\mu\text{m}$  of thickness. To accomplish this task, welding of AISI 316L stainless steel, Hastelloy C-276, tantalum, Ti6Al4V and Monel 400 superalloy have been developed in pure material and dissimilar combinations. The experiments lead to hermetic and sound laser welds in several geometries between these thin foils and also between thin and thick base metals.

Besides thermal processes accomplished by traditional lasers, another program has been developed where thermal effects can be absent in the region of interaction between laser focus and processed piece. This occurs when laser pulses of very short temporal length, in the order of femtoseconds ( $10^{-14}$  to  $10^{-13}$  s) are employed. After a development that allowed machining with optimized process parameters in dielectrics, a similar study has been made in metals. Using such technique very tiny structures has been produced on glasses, and these structures were used to build complex microfluidic devices constituted of microchannels, pumps, reservoirs, mixers and other elements. Such microfluidic devices have been developed in the Laser and Applications Center to be used in biochemistry and radiochemistry studies that are actually in progress at IPEN. Texturing surfaces of very thin sheets of titanium has

also been developed with femtosecond lasers with the aim to improve adhesion of polymers to produce hybrid structures that are used in many areas of modern engineering.

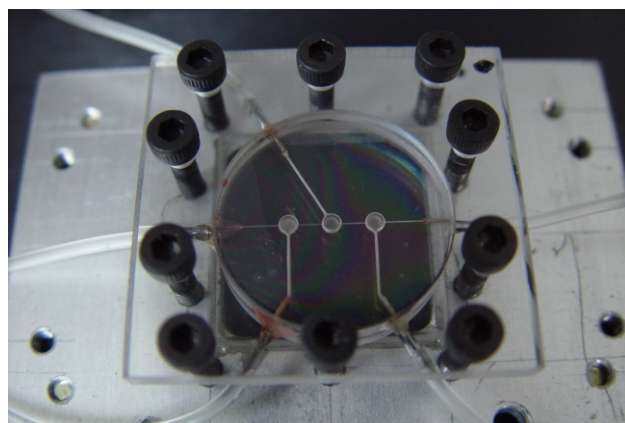


Figure 6. Microfluidic device machined with femtosecond laser pulses.

### Physical characterization of biological tissues for the development of new diagnostic and therapeutic methods

The physical characterization of biological tissues, mainly the study of their optical properties and thermal responses, allows the development of new processes using high intensity lasers, which can be useful as new diagnostic or therapeutic methods in Dentistry and Medicine. Protocol were developed and tested for several diseases. The caries prevention with laser was also studied in vitro and a clinical trial was carried out to prove the safety and effectiveness of the method. A cream for topical use for the clinical photodynamic therapy of skin cancer was developed, tested and patented in Veterinary Medicine. We are also studying the potential treatment of burned skin with high intensity femtosecond laser as well as the potential use of erbium laser to cut bone during surgery.

### Prevention of dental caries with lasers in vitro

The decline in dental caries over the last few decades has been attributed to the extensive use of fluoride. Although fluoride is the most powerful treatment to prevent tooth decay, the development of new methods to completely control this disease is still necessary, mainly in developing countries. In this way, lasers combined or not with fluoride, have been tested on teeth to improve dental enamel properties in order to enhance its resistance to demineralization.

We investigated the compositional and crystallographic changes in vitro on enamel when irradiated by Er,Cr:YSGG or Nd:YAG associated with black coating, its resistance to demineralization when irradiation is associated with fluoride, and  $\text{CaF}_2$ -like material formation and retention. Sample surfaces were analyzed by ATR-FTIR. Irradiation with Er,Cr:YSGG laser promoted a significant decrease on carbonate content of enamel. After Nd:YAG irradiation, it was observed a significant decrease of carbonate and amides I and II. X-ray diffraction measured at Synchrotron facility showed that both laser irradiations promoted formation of  $\alpha$ -tricalcium phosphate and tetracalcium phosphate, and a significant increase on the crystal growth of the enamel apatite. These changes can explain the improved resistance of enamel to demineralization observed in another study, in which enamel slices received professional fluoride gel applied before or after irradiation. Both lasers significantly reduced enamel demineralization, and the previous APF-gel application followed by laser showed the higher reduction of enamel demineralization.  $\text{CaF}_2$  formed before pH-cycling was significantly higher in groups were APF was associated with laser irradiation. After demineralization in vitro, these groups also presented higher  $\text{CaF}_2$  retention in respect to isolated treatments (only APF or only laser). The combined treatment of laser irradiation with fluoride propitiates an expressive fluoride uptake, reducing the progression of carieslike lesions, and this treatment is more effective than laser or fluoride alone.

### Prevention of dental caries with lasers – clinical trial

After all in vitro results described above, a double-blind crossover clinical trial was developed, in which 121 teeth of 33 volunteers were selected. In all volunteers, the right side teeth were selected for Nd:YAG laser + APF application (lased group) and the left side teeth were kept as control group (only APF application). Nd:YAG laser irradiated teeth painted with a black organic ink; after that, topical APF was applied. Recalls were made after 1 year in order to evaluate the formation of white-spot lesions or caries cavities. After 1 year, this clinical experiment showed an overall reduction of 60.2% in caries incidence in (lased group + APF) when compared with control (no treatment) and 39.2% of reduction when compared with only fluoride group. As a conclusion, combined Nd:YAG laser and topical fluoride treatment was effective for reducing the incidence of caries in vivo.

### Lasers in Periodontology – clinical trial

The Nd:YAG laser efficacy associated with conventional treatment for bacterial reduction has been evaluate after Nd:YAG laser irradiation was associated with scaling and root planning in class II furcation defects in patients with chronic periodontitis. Thirty-four furcation lesions were selected from 17 subjects. The control group received conventional treatment, and the experimental group received the same treatment followed by Nd:YAG laser irradiation. Both treatments resulted in improvements of most clinical parameters. A significant reduction of colony forming unit (CFU) of total bacteria number was observed in both groups. The highest reduction was noted in the experimental group immediately after the treatment. The number of dark pigmented bacteria and the percentage of patients with *Porphyromonas gingivalis*, *Prevotella intermedia*, and *Actinobacillus actinomycetemcomitans* reduced immediately after the treatment and returned to values close to the initial ones 6 weeks after the baseline for both groups. The Nd:YAG laser associated with conventional treatment promoted significant bacterial reduction in class II furcation immediately after irradiation, although this reduction was not observed 6 weeks after the baseline.

### Development of therapeutic processes of photosensitization and photobiomodulation

The aim of this activity is to develop new therapeutic processes using innovative technology through low-power lasers and light-emitting diodes to provide a nonthermal, noninvasive, environmental safe treatment that can be useful in the Health Sciences. The overall mission of this activity is to develop phototherapeutic processes for human health through of the physical, chemical and biological knowledge of the low intensity light tissue interaction. Our major interests are to investigate the effects of low intensity light therapy (LILT) and photodynamic antimicrobial therapy (PAT) on biosystems. More recently, application of nanomaterials in optical therapy and diagnosis were incorporated to our experiments.

### Photobiomodulation

LILT is a treatment modality that is becoming more useful in Health Sciences, although mechanisms underlying light effects are still not completely understood. Our group develops researches on light dosimetry and tissue optics to provide to the health professionals scientific background for using this technology to benefit patients. Studies are carried out in vitro and in vivo to investigate the influence of LILT on cell cultures, pain relief, wound healing, edema, and chronic inflammation. Our results show that LILT promotes a faster wound healing in obese mice and light parameters must be adjusted depending on body mass of individuals. Optical coefficients of biological tissues change depending on gender, strain and pigmentation of mice suggesting that absorption and scattering coefficients must be considered to optimize low intensity light therapy.

### Photosensitization

PAT is based on the application of a photosensitizer, a light source, and oxygen to kill microorganisms. PAT can be useful in life sciences, where along with conventional treatment provides a higher efficiency to care for local infections and tropical diseases. Alone, neither photosensitizer nor light has the capacity to produce deleterious effect on the biological system. However, when combined, they can eliminate bacteria, fungi, and protozoa, including those resistant to conventional drugs. Our results show that the effects of PAT on biofilms grown on dental tissue successfully reduced the survival of bacterial cells in biofilms; the use of PAT added to endodontic treatment in infected roots canals with optical fibre/diffusor is better than when the laser light is used directed at the access of oral cavity; PAT may inhibit virulence factors and reduce in vivo pathogenicity of *C. albicans* as well as antifungal drugs could be combined with PAT to treat *C. albicans* infections; PAT is a promising therapy for vaginitis since it is able to reduce fungal infection in biofilm and inflammatory signals in a murine model.

### Nanomaterials

Nanomedicine is developed to open new possibilities on research, prevention, and treatment of diseases through the innovative diagnostic imaging techniques and therapies. In this context, quantum dots (QD) are semiconductor nanocrystals and currently are being applied in bioassays that might be used in the diagnosis and therapeutic applications, such as photodynamic therapy, gene silencing, and drug delivery, as well as simultaneous diagnosis and treatment (theranostics).

On the other hand, antimicrobial effect of silver nanoparticles is related to its reduced size (about 13 nm), which allows them to interact closely with membranes and also to penetrate in microbial cell. Our results demonstrate that we have developed an effective bioconjugation of concanavalin A to CdTe/CdS quantum dots and have observed a specific labeling of saccharide-rich structures on *C. albicans* biofilm extracellular matrix and cell walls at hyphae and yeast morphologies. Besides, the association of silver-pectin nanoparticles to PAT mediated by riboflavin and blue light enhanced the bactericidal effect against *Streptococcus mutans*.

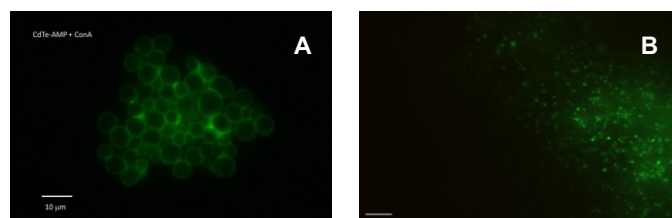


Figure 7. Fluorescence micrograph of fungal cells incubated with CdTe-AMP. An intense fluorescence of quantum dots is observed in the cell wall (A) and in fungal biofilm (B).

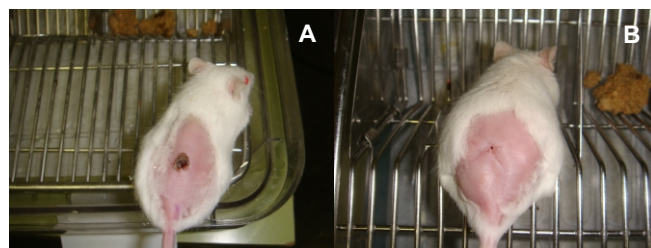


Figure 8. Low level laser therapy hastens skin wound healing in obese mice depending on light dosimetry. (A) Control group and (B) laser treated group 14 days after injury.

## Optical coherence tomography applications

Optical coherence tomography (OCT) is a diagnostic imaging technology based on low length coherence interferometry in which the coherence features of photons are explored, leading to an imaging technology that is capable of producing non-contact, non-destructive, high-resolution cross-sectional images of internal microstructures of living tissues. We implemented several OCT systems.

Innovative studies are being performed in order to make OCT a tool even powerful and flexible. The laboratory has studied the improvement of optical setup itself and also new ways of data analysis, such work provided interesting results in the period, and they are presented in the following paragraphs.

For instance it was prospected the possibility of using the autocorrelation signal to perform tomographic images (Au-OCT) of variety of sample kinds, showing that even samples with a complex structure, can be imaged by autocorrelation signal, since the first surface reflection has intensity enough to be used as a reference signal.

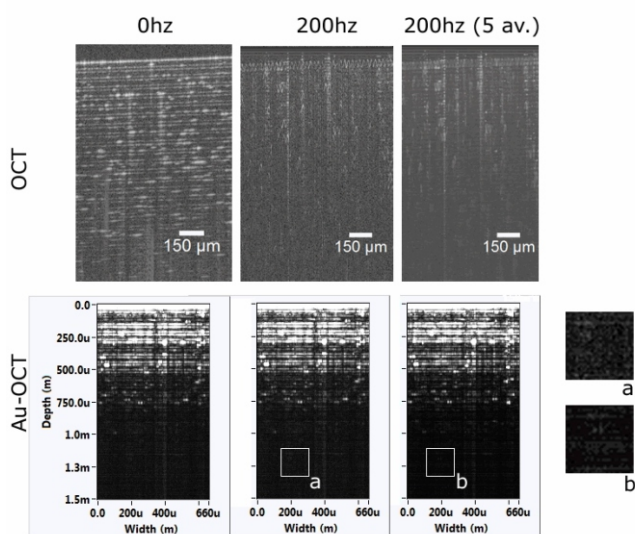


Figure 9. First row OCT image and at second row Au-OCT image. The first column shows the samples at rest, second column sample moves @200 Hz and the OCT exhibits morphological distortion while Au-OCT do not. At the last column sample moves @200 Hz and averaging of 5 a-scans were performed. The OCT image is blurred and the Au-OCT shows the same quality as the sample was at rest.

The laboratory also has proposed a new methodology which uses false structures, referred to as harmonics, to improve differential axial resolution in highly reflective samples, in this way was demonstrated that without any setup upgrade is possible, to certain configurations, improve OCT resolution by a factor three.

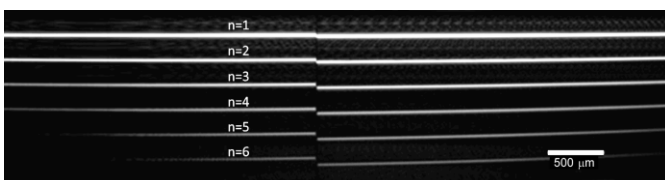


Figure 10. OCT image of a step height sample. The coherence length of the SLED gives the setup 6 μm resolution in air. The sample, in this case, has a 10 μm step.

Another interesting case was the work in which was possible to evaluated the characterization of tooth demineralization in incipient caries by analyzing the total optical attenuation coefficient obtained from the OCT data. This method allowed detection of demineralization with good performance.

Studies regarding the detection of flow are also being carried in the laboratory. Speckle, a form of coherent noise present in OCT, was shown to hold a time-dependent relation with regions of flow in the

sample being imaged, and have been used to generate maps of such regions.

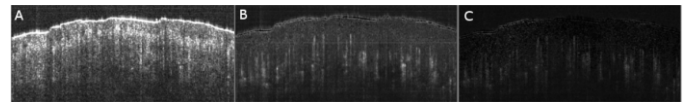


Figure 11. Example of regions of flow (brighter regions) identified in an OCT image of a finger. (A) Raw image. (B) Image after being analyzed with the autocorrelation method. (C) Image after being analyzed by Speckle Variance, the most common method.

## Lasers applications in nuclear science

Among the recently installed laboratories in IPEN is the Laboratory for Lasers Applications in Nuclear Science, which has the mission of help the nuclear field, with innovative ideas, to improve process efficiency, safety and security (environmental and individual).

As already known lasers are a very adaptive tool, making its applications very likely and helpful whatever the scenario, however some nuclear issues were picked to be tackled in this period, they are:

- 1) Laser assisted decontamination of surfaces impregnated with radioactive material;
- 2) Laser assisted deposition of thin films aiming the development of neutrons detectors and
- 3) Laser induced breakdown spectroscopy (LIBS) characterization of nuclear/radioactive material.

All these process have in common very high intensities of energy deposition via laser, making almost any kind of material evaporate instantly. For instance, surface contaminated materials can be, very effectively, decontaminated by the evaporation of the initial layer (nanometers), ejecting the contaminated material, which can be collected and stored. This process can be considered extremely environmental friendly when compared with chemical and abrasive approaches, mainly because its uses no inputs and has no outputs besides the contaminated material.



Figure 12. Laser decontaminated plate from a radioactive lightning rod. The thin powder at the bottom contains the contaminant and can be easily stored; the plate can then be recycled.

Efforts are also being made to develop a low cost small sized neutron detector, based in the  $^{10}\text{B}(n,\alpha),\text{Li}$  nuclear reaction. Using the laser is possible to evaporate and deposit a thin layer of natural boron over a photodetector (semiconductor). The resulting alpha can promote carriers to the conduction band, providing an electrical signal. Initial studies are being performed with ordinary materials, such as copper and silver, so the metallic boron can be processed.

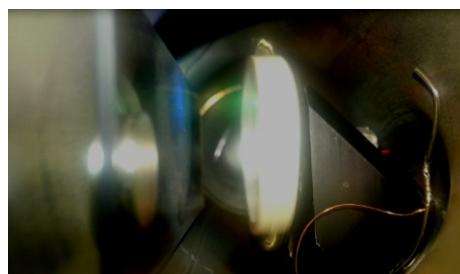


Figure 13. Photograph of the vacuum chamber, where a silver plate are been evaporated (greenish plume) by an infrared laser (invisible) and condensates on a glass slide (bluish area).



As a last highlight investigations of characterization of nuclear/radioactive materials via LIBS are being performed. The idea is to access the isotopic inventory optically. The pro of this methodology is to measure materials which do not emit gamma radiation strongly, allowing measuring its composition remotely. This technique is based in the spectral analysis of the plume formed when the laser ablates the material of interest. In order to do that, high technology systems and careful data analysis needs to be performed.

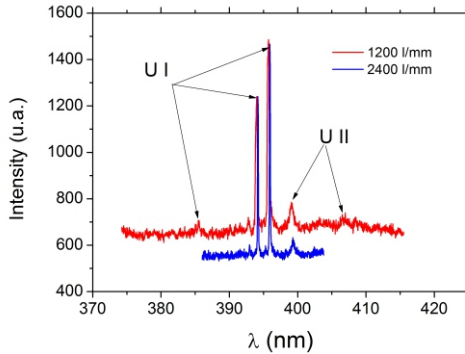


Figure 14. Optical spectrum of a nuclear fuel taken by LIBS technique - the peaks identifies the material of interest.

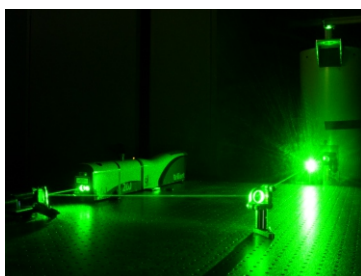
### Laser remote sensing of the atmosphere

LIDAR is the acronym for Light Detection and Ranging and like RADAR operates on the same principles of sending electromagnetic radiation into the atmosphere and detecting the returned light signal. This technique is powerful due its high temporal (seconds to minutes) and spatial (below 10 m) resolutions. With a few laser shots the system is able to characterize the atmospheric dynamics, the presence of pollutants and study dispersion patterns important features in pollution monitoring. Also this system is capable of tracing mid- and long-range transport of biomass burning activities in rural areas of the country. Also the LIDAR is an important climatological tool for studying cloud-base altitudes, water vapor atmospheric content and aerosol optical properties, which have been investigated since 2001, and the Laboratory of Environmental Laser Application was created. The LIDAR system at IPEN operated on physical principles of elastic scattering, namely Rayleigh and Mie scattering, and inelastic scattering, Raman scattering. The former is used to monitor aerosols in the atmosphere, and besides their optical properties, aerosols act as tracers for atmospheric dynamics and cloud formation.

The Raman channels in the system are used to perform water vapor, nitrogen and oxygen concentration profiling. Besides in a collaborative effort with Howard University and Goddard Space Flight Center - NASA we have developed an independent calibration methodology to obtain a vertical distribution of water vapor mixing ratio in the atmosphere based on physical principles.

The laboratory is nowadays responsible for 3 stations, one mobile and two fixed at São Paulo and Cubatão. There is a project to install a system in Natal for monitoring long range transport in cooperation with the PIC Institute in Moscow and University of Granada, Spain. More recently the LIDAR station was added to the WMO (World Meteorological Organization) as a coordinating station of the LALINET (Latin American LIDAR Network).

Figure 15. LIDAR system in operation at IPEN, which shows the second harmonic laser beam from Q-switched Nd:YAG laser.



### Operation and optimization of the TW peakpower laser and applications

High power ultrashort pulses lasers based on CPA (Chirped Pulse Amplification) technologies allow the study, in conventional laboratory scales, of phenomena that only 10 years ago were restricted to national laboratories with annual budgets of billions of dollars. In the Center for Lasers and Applications at IPEN, a hybrid Ti:Sapphire/Cr:LiSAF TW peak power laser system is under continuous development. A flashlamp pumping cavity for a Cr:LiSAF gain medium in the shape of a rod was built. The pumping cavity was developed aiming to minimize the thermal load on the Cr:LiSAF crystal by the use of absorption filters between the filters and the gain medium, allowing the amplification of ultrashort pulses to the terawatt peak power region at high repetition rates.

The pumping cavity was initially used in a laser configuration, and generated 60  $\mu\text{s}$  pulses with energy up to 2.8 J, with an average power of 30 W at 15 Hz repetition rate, the highest reported to date. The utilization of the pumping cavity in a hybrid Ti:Sapphire/Cr:LiSAF CPA system produced pulses with 30 mJ of energy and 60 fs of duration at 5 Hz repetition rate, reaching 0.5 TW of peak power, the highest in the southern hemisphere. Our laboratory also has another amplified laser system capable of generating up to 800  $\mu\text{J}$ , 25 fs pulses or 300  $\mu\text{J}$ , 5 fs pulses. Even at lower peak powers, the ultrashort character of the pulses generates nonlinear phenomena, particularly those initiated by multiphotonic and tunneling processes that generate free electrons.

Ultrashort pulses were utilized to ablate and machine technological materials with precision on the micrometer scales without heat affected zones, and to study how laser created defects (color centers, vacancies) affect the ablation dynamics in various material such as crystals. This nonthermal ablation is being studied for the removal of necrosed material from burned animals and its effects on the tissue regeneration. The Ultrashort pulses are also used to measure nonlinear effects in solid and liquid samples, and to synthesize metallic nanoparticles with controlled size, and high power pulses with tens of GW of peak power were used to create photons in the XUV spectral region using the High Harmonics Generation technique, in which ultrashort lasers pulses focused in a gas jet in vacuum originate pulses with durations in the attosecond regime.

### Determination of ultrashort pulses ablation thresholds of solid samples and applications to micromachining

The ablation of solids by ultrashort pulses is due to a Coulomb explosion following the ejection of surface electrons accelerated by the laser electric field, or by a phase explosion resulting from in a high density of free electrons generated by avalanche ionization. The pulses very brief duration, shorter than the typical phonon period, mainly heats the electrons and the explosions that remove material occur after the pulse has finished, with minimal material heating. The avalanche occurs when seed electrons, either already present in metals or created by tunneling or multiphoton ionization in other materials, are accelerated by the ultrashort pulse electric field into a quivering motion and generate more free electrons by impact ionization in an exponential growth process that is almost independent of the material being irradiated. The high intensities reached by ultrashort pulses easily induce the nonlinear phenomena that create the initial free electrons, making these pulses efficient tools to etch any kind of material. Due to this nonselective mechanism, the only parameter that has to be known to etch a material with ultrashort pulses is its ablation threshold fluence,  $F_{th}$ . This ablation threshold derives from the material atoms bonding energies, electronic density and its ionizing energies, which depend on the presence of dopants, impurities or other defects. As a consequence of the defects presence, the seed electrons are created more easily and the avalanche ones are freed at lower impact energies, decreasing the  $F_{th}$  value. These defects can be created by ultrashort laser pulses, and in this case the modifications induced by a pulse modify the  $F_{th}$  value for the following pulses, until the defects density reaches saturation and  $F_{th}$  stabilizes at a constant value. These cumulative phenomena are known as incubation effects, and the

ablation threshold fluency modifications caused by them must be taken into account when machining a material.

A few years ago we introduced a simple experimental technique, which we denominated D-Scan (Diagonal Scan), to quickly measure the ultrashort pulses ablation threshold of a solid sample. Recently we modified this technique to allow the ablation threshold measurement for an arbitrary pulse superposition, and the consequently determination of the incubation effects. Knowing the ablation threshold for the superposition of multiple pulses is important when machining samples with ultrashort pulses, in which the sample displacement speed and laser repetition rate play an important role in setting the pulses overlap, and determine the morphology and quality of the structures etched. Our technique presents advantages over the traditional one due to its speed and for also reproducing the machining conditions more closely.

Using the results obtained for the superposition of many pulses, new methods were developed to etch structures in the surfaces of technological materials minimizing the material modifications on the neighborhood of the etched regions.

### Synthesis of metallic nanoparticles with controlled dimensions

Ultrashort laser pulses were used to synthesize silver and gold nanoparticles controlling its size. Starting from colloidal salt solutions containing capping agents, these were illuminated by blue light that neutralizes the metallic atoms, which aggregate into clusters. The solutions containing the clusters were then irradiated by ultrashort pulses, which, through photolysis, break the clusters into smaller nanoparticles. We have found that controlling the pulse duration and its relative spectral phase is possible to determine the final nanoparticles average size and its dispersion. This method is now being improved in order to allow the synthesis of the nanoparticles controlling its geometry, enabling the production of spheres, rods, prims and on the nanoparticles shapes, thorough the use of an optical control feedback by analysis of the nanoparticles solution absorption spectra and a genetic algorithm.

### Generation of high harmonics into the VUV and soft X-ray spectral regions

When a high intensity ultrashort pulse impinges on a gas at low pressure, electrons can be freed from its parent atoms by the leading of the pulses, and then be accelerated by the pulse carrier wave into a quivering motion, acquiring kinetic energy. When these electrons collide with the atom, their energy is released in the form of odd harmonics of the exciting field, and if the kinetic energy is sufficiently high, the harmonics can reach the UV and soft X-ray region, generating photons up to a few keV. In the High intensity ultrashort pulses laser laboratory, we are pursuing the generation of these harmonics into the region of the water window, around 2-4 nm, which are proposed to be used in high-resolution radiographies of living tissues. Using 25 fs pulses focused into a gas (Argon) jet inside a vacuum chamber, we generated harmonics up to 30 eV (40 nm), into the XUV spectral region. The experimental apparatus is being improved, and the generation mechanisms are under study to allow us to generate more energetic photons into the soft X-ray region.

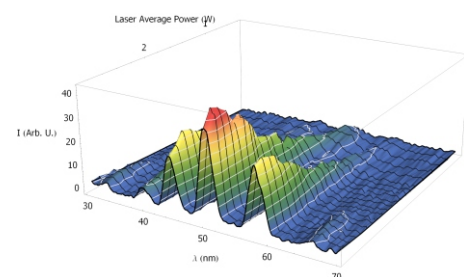


Figure 16. Spectra of the harmonics generated in the XUV region, showing its dependence on the laser average power.

### Research Staff

Dr. Anderson Zanardi de Freitas; Dr. Denise Maria Zzell; Dr. Eduardo Landulfo; Dr. Gessé Eduardo Calvo Nogueira; Dr. Izilda Marcia Ranieri; Dr. Laercio Gomes; Dr. Marcus Paulo Rael; Dr. Martha Simões Ribeiro; Dr. Niklaus Ursus Wetter; Dr. Nilson Dias Vieira Junior; Dr. Ricardo Elgul Samad; Dr. Sonia Licia Baldochi; Dr. Wagner de Rossi; Tech. Jose Tort Vidal; Tech. Marco Antonio Andrade; Tech. Marta de Jesus Silva; Tech. Paulo Cesar da Silva; Tech. Solange Eiko Mitani; Tech. Tito de Deus; Tech. Valdir de Oliveira; Suely Tavares Venancio.

### Graduate Students

Alessandra Baptista; Alessandro Nogueira; Ana Claudia Ballet de Cara; Anderson Pimentel Damian; Andrea de Avilez Calmon Nogueira da Gama; Antonio José da Silva Santos; Antônio Carlos Martinho Junior; Arthur Máximo; Caetano Padiál Sabino; Claudia Bianchi Zamataro; Claudia Strefezza; Claudir Giannetto; Carolina Benetti; Cassio Aparecido Lima; Cedric Sebastien Martins Figueiredo; Cristine Calil Kores; Danilo Mariano da Silva; Débora Picanço Aureliano; Denilson Camargo Mirim; Eduardo Spinelli; Fabio Cavalcanti; Felipe Vasconcelos Araujo; Fernando Rodrigues da Silva; Gerson Hiroshi de Godoy Nakamura; Guilherme Henrique Dias; Henrique Coli Schumann; Horácio Marconi da Silva Matias Dantas Linhares; Ivanildo Antônio dos Santos; Jair Ricardo de Moraes; Jana Carine Guimarães Espósito; Jonas Jakutis Netto; José Quinto Junior; Leandro Matioli Machado; Lidia Ernestina Santana; Lucas Ramos De Pretto; Lúcia de Fátima Cavalcanti dos Santos; Luis Claudio Suzuki; Marcello Magri Amaral; Marcus Paulo Rael; Marcia Talita Amorim Marques; Maira Franco de Andrade; Mariana Tiemi Iwasaki; Marcelo Noronha Veloso; Mariella da Silva Gottardi; Mario André Prieto Aparício Lopez; Matheus Araujo Tunes; Melissa Santos Folgosi-Corrêa; Moisés Oliveira dos Santos; Patricia Ferrini Rodrigues; Paulo Roberto Correa; Renata Facundes da Costa; Renato Juliani; Regiane de Souza Pinto; Rosa Maria Machado de Sena; Saara Maarit Reijn; Selly Sayuri Suzuki; Tania Mateus Yoshimura; Thiago Martini Pereira; Viviane Pereira Goulart; Willian Caetano Rodrigues.

### Co-Workers

Dr. Adriana da C. Ribeiro; Dr. Adriana Ramos de Miranda; Dr. Alessandro Melo Deana; Dr. Ana Maria do Espirito Santo; Dr. Anderson S. L. Gomes; Dr. Anderson Stevens Leonidas Gomes; Dr. Adriana Bona Matos; Dr. Adriana C. Ribeiro; Dr. Andrea Moreira; Dr. Aginaldo Silva Garcez; Dr. Alexandros Papayannis; Dr. André Felipe Henriques Librantz; Dr. Andre Rolim Baby; Dr. Antonio Martins Figueiredo Neto; Dr. Carlos de Paula Eduardo; Dr. Christian Apel; Dr. Cid Bartolomeu de Araujo; Dr. Claudio Oller; Dr. Claudete Rodrigues Paula; Dr. Cristiane Miranda França; Dr. Daniela de Fátima Teixeira da Silva; Dr. Daniel Milanese; Dr. Dario Santos Junior; Dr. David Whiteman; Dr. Demetrius Venable; Dr. Detlef Klimm; Dr. Dimitri Geskus; Dr. Eliane Gonçalves Lorena; Dr. Eriques Gonçalves da Silva; Dr. Francisco José Krug; Dr. Gerhard Held; Dr. Giorgio de Micheli; Dr. Giorgos Giorgoussis; Dr. Helen Pask; Dr. Igor Veselovskii; Dr. Isabela Capparelli Cadioli; Dr. Janaina Merli Aldrigui; Dr. Jean Jacques Zondy; Dr. John Girkin; Dr. Julia Maria Giehl; Dr. Juliana Sayuri Kimura; Dr. Lilia Coronato Courrol; Dr. Luciano Bachmann; Dr. Marcia Pinto Alves Mayer; Dr. Márcia P. A. Mayer; Dr. Márcia Turolla Wanderley; Dr. Marcos Pinotti Barbosa; Dr. Maria de Fátima Andrade; Dr. Maria Valeria Robles Velasco; Dr. Maria Paulete M.P. Jorge; Dr. Mario Ernesto Giroldo Valério; Dr. Mark Vaughan; Dr. Mauricio Baptista; Dr. Michael Hamblin; Dr. Norbert Gutknecht; Dr. Orlando Parise Jr.; Dr. Paulo Sergio Fabris de Matos; Dr. Patricia A. da Ana; Dr. Philippe Keckhut; Dr. Piero Zanardi; Dr. Renato Araujo Prates; Dr. Roberto Guardani; Dr. Sheila Cristina Gouw-Soares; Dr. Silvia Cristina Núñez; Dr. Spero Penha Morato; Dr. Stuart D. Jackson; Dr. Taciana Toledo; Dr. Thiago da Silva Cordeiro; Dr. Vicente Afonso Ventrella; Dr. Walter Movinobu Nakaema; Dr. Walter Velloso.

### Honor Mention and Awards

Caetano Padiál Sabino, Martha Simões Ribeiro - “Estudo da atenuação da radiação laser em tecidos biológicos: influência da cor e processo inflamatório” - Best Poster Award, PIBIC - IPEN/CNEN-SP, 2011.

Ricardo Elgul Samad - “II Prêmio de Fotografia - Ciência e Arte” - Best Photography (second place), CNPq, 2012.

Gesse Eduardo Calvo Nogueira - “17th World Congress on Dental Traumatology” - Silver Award in the category Diagnosis and Treatment Technique, Rio de Janeiro, 2012.

Caetano Padiál Sabino, Martha Simões Ribeiro - “Modelo de estudo in vitro de infecções por biofilme de *Candida albicans* e sua inativação por terapia fotodinâmica” - Best Oral Presentation Award, PIBIC - IPEN/CNEN-SP, 2013.

Martha Simões Ribeiro was honored due to its valuable academic work contribution in the triennium 2010-2013 - “Comissão de Pós-Graduação do Programa de Tecnologia Nuclear”, IPEN/USP, 2013.

Martha Simões Ribeiro - “Photodynamic effect of riboflavina associated with silve pectin-nanoparticles in *Streptococcus mutans*” (honor mention), XXVIII Reunião Anual da FeSBE - Federação de Sociedades de Biologia Experimental, 2013.